

Two-photon excited LIF determination of H-atom concentrations near a heated filament in a low pressure H₂ environment

Ulrich Meier, Katharina Kohse-Hoinghaus, Lothar Schafer, and Claus-Peter Klages

With respect to the investigation of low pressure filament-assisted chemical vapor deposition processes for diamond formation, absolute concentrations of atomic hydrogen were determined by two-photon laser-induced fluorescence in the vicinity of a heated filament in an environment containing H₂ or mixtures of H₂ and CH₄. Radial H concentration profiles were obtained for different pressures and filament temperatures, diameters, and materials. The influence of the addition of various amounts of methane on the H atom concentrations was examined. *Keywords:* Two-photon laser-induced fluorescence, atomic hydrogen, quantitative concentration measurements, hot filament CVD of diamond.

1. Introduction

Due to the attractive physical properties of diamond, its growth by chemical vapor deposition (CVD) is a technical process of considerable importance. Successful techniques for low pressure diamond formation were reviewed in several recent publications.^{1,2} The mechanisms of diamond growth are far from being thoroughly understood. Of crucial influence on the rate and quality of diamond formation appears the presence of atomic hydrogen³ and of one or more hydrocarbon precursors, e.g., methyl or acetylene. The role of atomic hydrogen seems to be at least threefold¹⁻³: H atoms tend to stabilize favorable *sp*³ bonds at the carbon surface; their rate of etching graphitic or amorphous carbon is faster than that of etching diamond; and they might support the gas phase formation of suitable diamond growth species. High H-atom concentrations, even above thermal equilibrium, have been postulated for efficient diamond formation.³

In situ monitoring of stable and active species in the CVD formation process might contribute to further insight into the diamond growth mechanism and thus to the design and development of improved technical procedures. To date, only a limited number of investigations provide this kind of information. Infrared absorption spectroscopy⁴ and mass spectrometry⁵ have recently been used to detect several hydrocarbon species of interest in typical environments for filament-assisted CVD diamond growth. Atomic hydrogen has been monitored by resonance enhanced multi-

photon ionization (REMPI).⁶ Although this study has provided radial profiles of H atom REMPI signals, it is not clear how the measured profiles correspond to absolute concentrations of atomic hydrogen.

In the present investigation, two-photon laser-induced fluorescence (LIF) was used to determine quantitative H-atom concentrations. Hydrogen atoms were excited to the *n* = 3 state by simultaneous absorption of two photons at 205 nm and detected by observation of the subsequent fluorescence to the *n* = 2 state at 656 nm. The calibration procedure for the determination of absolute atom concentrations was successfully applied in combustion related experiments.⁷⁻⁹ It is based on known atom concentrations in a discharge flow reactor. Fluorescence signals obtained in the discharge flow reactor are correlated to the ones measured under identical excitation and detection conditions in the system under investigation. As the fluorescence is subject to quenching, the effects of different pressure, temperature, and chemical composition in the two systems have to be accounted for in the calibration. Quenching coefficients for a variety of collision partners have been measured in a previous study.¹⁰

With this technique, quantitative concentration profiles of atomic hydrogen have been measured in a low pressure hydrogen environment in conditions typically found in diamond growth experiments²: filament temperatures between 2000 and 2500 K; distances from the filament up to 28 mm, and pressures of 1.5–100 mbar with up to 5% CH₄. The H-atom concentrations were determined as a function of several important parameters as filament temperature, material, diameter, and overall pressure. Also, the effect of methane addition has been studied. Preliminary results have already been presented.¹¹ This report mainly focuses on the diagnostic technique and addresses the key results. The technical relevance of these results is discussed elsewhere.¹² Since this study was performed specifically with the aim of demon-

Ulrich Meier and K. Kohse-Hoinghaus are with DLR Institute for the Physical Chemistry of Combustion, D-7000 Stuttgart 80, Federal Republic of Germany; the other authors are with Philips GmbH Hamburg Research Laboratory, D-2000 Hamburg 54, Federal Republic of Germany.

Received 13 March 1990.

0003-6935/90/334993-08\$02.00/0.

© 1990 Optical Society of America.

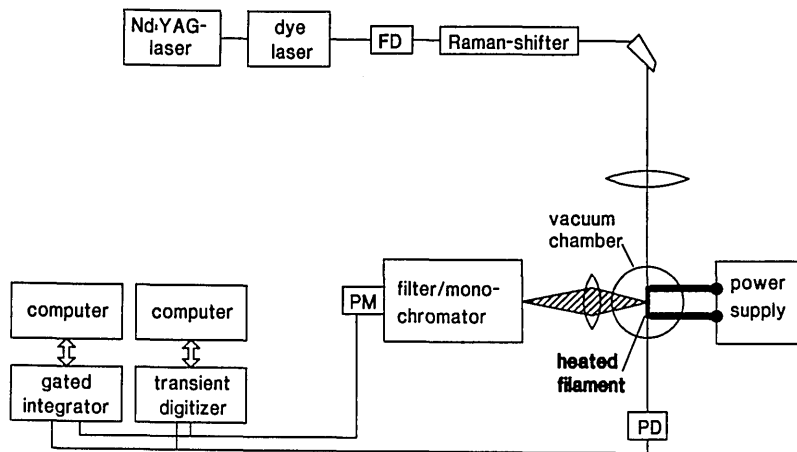


Fig. 1. Experimental arrangement: *PD*, photodiode; *PM*, photomultiplier; *FD*, frequency doubling crystal.

strating the applicability and potential of two-photon laser excited fluorescence as a quantitative diagnostic tool for the investigation of gas phase effects in typical experimental diamond growth conditions, no attempt was made to produce diamond films. Hence, no substrate was included in the experimental arrangement.

II. Experimental

Figure 1 shows the experimental arrangement. For the two-photon excitation of hydrogen atoms, a Nd:YAG pumped frequency doubled dye laser running on a mixture of fluorescein 27 and rhodamine 6G at ~ 551 nm was used; its output was shifted to 205 nm using the third-order anti-Stokes Raman line in hydrogen. The pulse energy was ~ 50 μ J. The laser radiation was then focused into the vacuum cell parallel to the filament with a $f = 150$ -mm lens; the resulting focal diameter, which determined the radial spatial resolution, was 250 μ m, corresponding to a power density of ~ 25 MW/cm². The filament was heated using a constant current power supply; the power delivered to the filament was electronically controlled to maintain an approximately constant temperature during an experiment. The fluorescence was passed through an interference filter or a monochromator; in the latter case, an image rotating optics was used to generate an image of the laser beam collinear with the entrance slit of the monochromator. Spatial H atom distributions could be measured by translating the heated wire with respect to the fixed excitation/detection arrangement. The spectrally filtered fluorescence was recorded by a photomultiplier (Hamamatsu R928) and further processed using either a boxcar integrator (Stanford Research Systems SR250), which measured temporally integrated signals, or a transient digitizer (Tektronix R7912), which was used for peak intensity and time-resolved measurements. The laser power was monitored with a photodiode, and the fluorescence signals were scaled with respect to the laser intensity corresponding to the quadratic dependence in the case of a two-photon excitation process.

Initial experiments showed that once the wire had reached a temperature at which it started to produce detectable amounts of H-atoms, it became so bright that its broadband radiation saturated the photomultiplier when using an interference filter of ~ 2 nm FWHM. Therefore, background discrimination had

to be improved using a monochromator with a bandwidth of ~ 0.18 nm. The interference filter, however, was better suited for the calibration experiments in the discharge flow reactor, since here the background emission was negligible.

For pressures below 10 mbar, the fluorescence lifetime was sufficiently long to allow determination of the quenching rate from time-resolved signals. Above 10 mbar, the temporal shape of the signals was determined by the shape of the laser pulse and the temporal response of the detection system; in this regime, integral signals were recorded using the boxcar integrator, and quenching rates were calculated from H₂ density and an independently measured quenching rate coefficient for H ($n = 3$) by H₂ (see below).

III. Results and Discussion

A. Calibration

The determination of absolute concentrations was based on a calibration of the H-atom fluorescence signals using reference measurements in a discharge flow reactor. This procedure had been applied earlier in the case of flame investigations.⁸ To make the signals comparable, the experiment was designed to allow replacement of the filament setup by the discharge flow reactor while all other components were maintained unchanged. In particular, the excitation/detection geometry and efficiency of the detection system were identical for both setups.

Hydrogen atoms were generated in the flow reactor by dissociation of H₂ diluted in helium in a microwave discharge. The flow reactor was typically operated at pressures between 2 and 10 mbar; the total flow rate was 2 slm. One percent hydrogen was added to the He carrier flow, resulting in H-atom concentrations of $1\text{--}2 \times 10^{15}$ cm⁻³; they were determined using the titration reaction $\text{H} + \text{NO}_2 \rightarrow \text{OH} + \text{NO}$. The fluorescence signal as a function of NO₂ concentration exhibited a linear decrease, as shown in Fig. 2. The intercept of the straight line with the abscissa yields the concentration of NO₂ necessary to remove a H-atom concentration corresponding to an intensity given by the ordinate intercept. Since the reaction of H-atoms with NO₂ is very fast, it is virtually completed within the upstream section of the flow tube in the usual operating conditions of the reactor. Therefore, the loss of

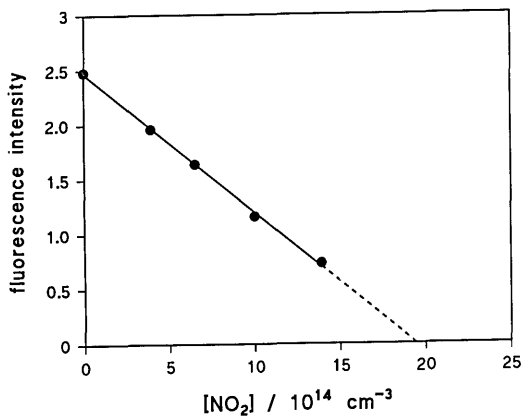


Fig. 2. Calibration curve for H-atom fluorescence signal. The NO₂ concentration at the abscissa intercept as given by the extrapolated straight line is equal to the H atom concentration corresponding to the signal intensity at the ordinate intercept.

hydrogen atoms due to wall recombination along the tube has to be taken into account, since the concentration at the detection point at the downstream end is lower than the initial concentration upstream. This was achieved by determining the wall recombination coefficient from measurements of relative H-atom signals as a function of flow velocity in the tube. The wall loss depends on flow conditions and was usually ~20%.

The concentration in the filament experiment [H]_{CVD} can be determined from the ratio of the fluorescence intensities I_{CVD} and I_{DFR} in the CVD and the discharge flow reactor, respectively, and the reference concentration [H]_{DFR} in the flow reactor:

$$[H]_{CVD} = [H]_{DFR} \times C_Q \times C_D \times I_{CVD}/I_{DFR}$$

In this evaluation it is assumed that no significant concentrations of atoms are produced by laser photolysis. To ensure this, the laser power density was kept as low as possible. Investigations both at room temperature⁷ and in H₂/O₂/Ar flames⁸ showed no evidence for production of H-atoms from photodissociation of H₂, even at higher laser powers. Also, no H-atom signal was found that could be contributed to CH₄ photolysis.

The scaling factor C_Q accounts for quenching effects and will be discussed in more detail in the following section. C_D is a correction factor which originates from the fact that the Doppler width of the H-atom absorption line becomes larger than the laser bandwidth at the high temperatures in the CVD experiment. The Rabi frequency Ω and hence the rate of a two-photon transition is a function of the frequency detuning δ , i.e., the difference between the laser and the atomic transition frequency¹³: $\Omega = \Omega(\delta)$. If this detuning is caused by the Doppler shift due to the thermal motion of the H-atoms, the Rabi frequency at a given temperature can be obtained by integrating over all possible values of the detuning δ , weighted by the normalized distribution function $D(\delta)$:

$$\Omega = \int_{-\infty}^{+\infty} \Omega(\delta) \times D(\delta) d\delta.$$

In the case of Doppler broadening $D(\delta)$ is given by

$$D(\delta) = 2/\nu_D \times \sqrt{\ln 2/\pi} \times \exp\{-\ln 2 \times [\delta/\nu_D]^2\},$$

with $\nu_D = \nu_0/c \times 2\sqrt{2 \cdot R \cdot \ln 2} \times \sqrt{T/m}$ (Doppler width), where R is the gas constant, ν_0 is the center frequency, and m is the molar mass.

The different values of Ω in the flow reactor and at the filament lead to varying excitation rates in the two systems. The factor C_D can be determined from the corresponding values of Ω using the procedures described earlier.⁷⁻⁹ For an average laser bandwidth of 1.5 cm⁻¹ and gas temperatures in the range of 1200–2500 K, the correction factor C_D ranged from 1.18 to 1.37, i.e., varied by 15%.¹⁴ Since this is in the same range as the uncertainty in C_D resulting from the determination of the laser bandwidth, we used an average value of 1.27, neglecting the small variation over individual profiles.

B. Quenching

The fluorescence quantum yield for H($n=3$) atoms is given approximately by the expression $A_3/(A_3 + Q_3 + W_{3i})$, where A_3 , Q_3 , and W_{3i} are the rates for spontaneous emission, quenching, and photoionization, respectively, out of the $n=3$ state. Given the cross section for photoionization of H atoms out of the $n=3$ state,¹⁵ the photoionization rate is between 1 and 2 orders of magnitude smaller than the quenching rate for the laser power density applied in these experiments, depending on pressure. In addition, its influence on the calculation of the absolute concentrations is taken into account in the calibration procedure.⁹ Depletion due to stimulated emission^{16,17} has been neglected here, since the power densities and hence the populations in the excited state were relatively low. Although stimulated emission can be very intense, it could not be observed in both the flow reactor and in the filament setup. In addition, since the populations in the excited state were comparable in the two systems, the influence of this effect is largely reduced by the calibration procedure.⁹ The Q_3 is different in the flow reactor and in the filament experiment due to different pressures, temperatures, and gas compositions; furthermore, it changes within the latter system as a function of pressure and temperature. Measurements were performed at pressures between 1.5 and 100 mbar; the temperatures ranged from 2300 K near the filament surface to ~1000 K at 28-mm distance (see below). A scaling factor has to be introduced to account for varying loss of quantum yield. The scaling factor can be obtained from numerical solutions of the set of coupled differential equations which describe the temporal evolution of the populations in the atomic states involved; this calculation has to be performed with values for Q_3 according to the pertinent experimental conditions. C_Q is then given by the ratio of the calculated peak intensities resulting from different quenching rates for a fixed total number density. Details of the procedure are reported elsewhere.⁹

For sufficiently low pressures, Q_3 can be obtained directly from measured lifetimes t_3 , which are related to the quenching rate by $1/t_3 = A_3 + Q_3$. In situations where the lifetime was too short to be measured directly, Q_3 was calculated from number densities $[M]$ of the collision partner M and independently measured quenching rate coefficients k_M according to $Q_3 = k_M(T)$

$\times [M](T)$. For a variety of collision partners, $k_M(T)$ has been measured in an earlier study.¹⁰ In the flow reactor, quenching could be neglected due to the low concentrations and the very low rate coefficient for the dominant collision partner helium. In the filament experiment, the quenching rate was mainly determined by collisions with H_2 . Even for the highest CH_4 additions, the contributions of methane to the quenching rate was below 20%.

Rate coefficients for quenching of H ($n = 3$) by H_2 showed only weak temperature dependence between 300 and 700 K.⁷ In addition, a crude estimate of the quenching rate coefficient derived from time-resolved measurements at the lowest pressures in the filament experiment of $1.2 \times 10^{-9} \text{ cm}^3/\text{s}$ was in fairly good agreement with the room temperature value of $2 \times 10^{-9} \text{ cm}^3/\text{s}$.⁷ Furthermore, as a consequence of the relatively high spontaneous emission rate, the scaling factor C_Q depends only weakly on the quenching rate for most of our experimental conditions. Therefore, we adopted the room temperature quenching rate coefficients even for the high temperatures in the CVD experiment.

Besides a potential temperature dependence of the quenching rate coefficient, the temperature influences the effective quenching rate to a larger extent via the density $[M]$ of the collision partner. Therefore, knowledge of at least approximate spatial temperature distributions is required. Filament temperatures at given electrical powers were calibrated with a two-wavelength pyrometer.¹² Corresponding temperature profiles were calculated¹⁸ using a model developed by Blodgett and Langmuir,¹⁹ which describes the heat transport from a hot wire to a gas. For these calculations some simplifying assumptions were made: It was assumed that the heat transport by hydrogen atoms was the same as that for an identical concentration of molecular hydrogen; also, heat release due to recombination was disregarded. These assumptions are justified by the generally low relative H atom concentrations. Also, since no data for the accommodation coefficient of H atoms on tantalum were available, a value pertinent to tungsten was adopted.¹⁹ The calculated temperatures can be compared to thermocouple measurements by Harris *et al.* in similar conditions.⁵ Although the volume flow rate in the measurements in Ref. 5 was lower than in this work (100 sccm) and another filament material was used, the temperatures agree with the thermocouple measurements usually within 100° except at positions very close to the wire, where the measured temperatures were lower. The filament diameter in Ref. 5 is not given; different filament diameters can account for different temperatures near the wire.

For filament temperatures of ~ 2550 K, calculations showed that for pressures above 10 mbar, gas temperatures decreased from ~ 2300 K at a 0.4-mm distance from the filament to 1000–1200 K at 28 mm, depending on pressure. For lower pressures, the gradient between filament and gas temperatures was steeper, but the decrease of temperature with distance was less distinct. At 1.5 mbar and a filament temperature of 2640 K, the gas temperature was 1750 K at 0.4-mm

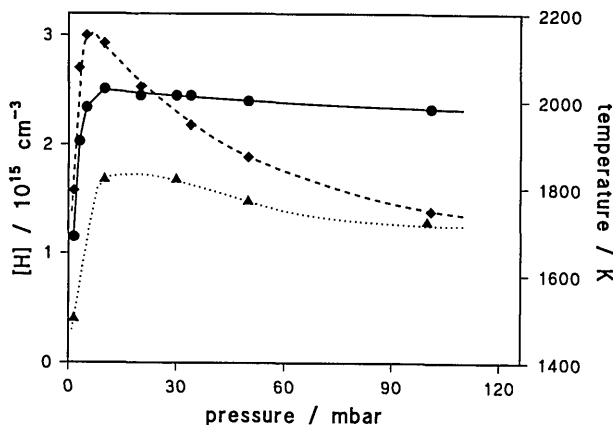


Fig. 3. Fluorescence signal (---◆---) and H-atom concentration (—●—) as a function of pressure in the CVD reactor; tantalum filament, 2-mm diameter, $T = 2540$ K; ...▲...: calculated temperature at measurement point (right ordinate).

distance, dropping to 1150 K at 28 mm. These temperature gradients led to relative corrections due to quenching of 25% or less over a spatial H-atom profile.

C. Concentration Measurements

Figure 3 shows fluorescence signals and H-atom concentrations as a function of pressure at a distance of 4.4 mm from the filament and a total H_2 flow rate of 750 cm^3/min . The experiment was performed using a tantalum filament 2 mm in diameter. The qualitative shape of the two curves is markedly different due to the decreasing quantum yield at higher pressures, resulting from the increasing quenching rate. Most filament-assisted CVD experiments are performed at pressures around 30 mbar or higher; this corresponds to a region where the initial steep increase of atom concentrations is well terminated and the H-atom density depends only weakly on pressure. The absolute concentrations correspond to a degree of dissociation of ~ 1 –4% at pressures above 30 mbar and $\sim 10\%$ at 10 mbar. The concentrations exceed values corresponding to thermal equilibrium based on the temperature at the respective positions rather than the filament temperature.

Given the statistical and systematic errors in the scaling factors C_Q and C_D , which are temperature dependent and in the calibration, respectively, the uncertainty of the absolute concentrations is a factor of ~ 2 . The temperature sensitivity of C_D is relatively low; it changes by only 13% between 1000 and 2000 K for our laser bandwidth. For the same temperature variation, the change in C_Q is 25%. Both corrections increase the H-atom concentration with decreasing temperature. The uncertainties in the relative concentrations for measurements at the same pressure are mainly given by the statistical error due to signal fluctuations, which was usually $\pm 10\%$.

In Fig. 4 radial concentration profiles are shown for some of the pressures from Fig. 3. For clarity, data taken at 100 mbar are not shown here; however, they basically coincide with the points at 10, 30, and 50 mbar, respectively. It can be seen that the weak dependence of the H-atom concentration on pressure in

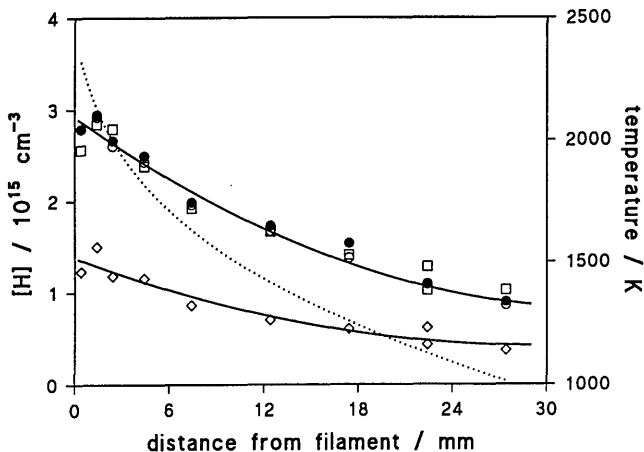


Fig. 4. Radial concentration profiles at different pressures: tantalum filament, 2-mm diameter: \diamond , 1.5 mbar, $T = 2640$ K; \circ , 10 mbar, $T = 2575$ K; \bullet , 30 mbar, $T = 2540$ K; \square , 50 mbar, $T = 2530$ K. Dotted line, temperature profile for 30 mbar; the temperatures for 10 and 50 mbar were similar.

the range above 10 mbar states in Fig. 3 is valid at all distances from the filament between 0.4 and 28 mm. In addition, even in the regime of higher pressure dependence, an increase in pressure of a factor 6.7 leads to atom concentrations higher by only a factor of 2.

H-atom number densities depend much more strongly on filament temperature than on pressure. Figure 5 shows radial concentration profiles for three different filament temperatures at a pressure of 30 mbar. In this case, no methane was added. It can be seen that the number densities show a very distinct increase with temperature. In particular, a threshold behavior for the formation of H-atoms was found: Below ~ 2000 K the concentrations were below our detection limit of $\sim 10^{13}$ cm $^{-3}$; above this temperature, a sudden increase of H-atom signals could be observed. The temperature dependence of the measured H-atom concentrations found in this work corresponds approximately to the dependence of equilibrium concentrations on temperature. In two former studies^{6,20} where relative H-atom concentrations have been measured, a somewhat weaker temperature dependence has been found. In this work only a limited temperature range could be investigated, since the detection sensitivity of the experiment did not allow concentration measurements at lower temperatures. To broaden the basis for a comparison, these results suggest future experiments over a wider temperature range with an improved experimental arrangement.

Since diamond deposition is discussed to be favored by a hydrogen superequilibrium,³ it is evident that in a filament process high temperatures are desirable. This leads to the necessity of selecting filament materials which are chemically stable in a reactive environment even at very high temperatures.

Within the scope of practical applications of the filament technique, the diameter of the wire used is another interesting parameter with respect to dissociation efficiencies. Figure 6 shows radial concentration profiles for three different filament diameters. The experiment was performed at a pressure of 30 mbar

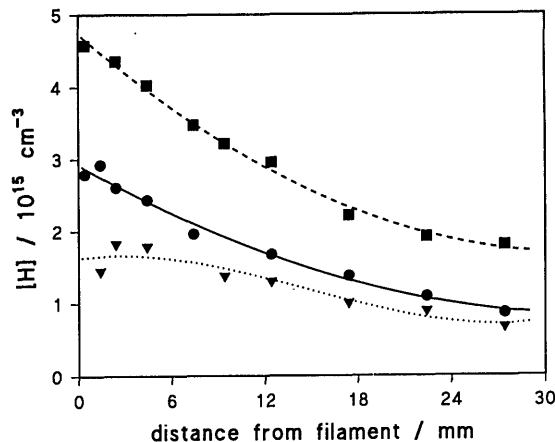


Fig. 5. Radial concentration profiles at different filament temperatures: --- \blacksquare ---, $T = 2620$ K; — \bullet —, $T = 2540$ K; ... \blacktriangledown ..., $T = 2450$ K. Tantalum filament, 2-mm diameter; $p = 30$ mbar.

and 5% CH $_4$ added. The electrical power supplied to the wire was adjusted to keep the filament temperature approximately constant for all three diameters. As can be expected intuitively, the concentration of H atoms produced by dissociation increases with the surface area of the filament. However, the dissociation efficiency does not scale with diameter. An increase of filament diameter of almost a factor of 7 results in an increase of the atom concentration of only a factor of 3.5 (extrapolated to the surface), if the data for 0.3 and 2 mm are compared. Our results concerning the dependence of H atom concentrations on filament radii do not support an increased dissociation efficiency for thinner filaments reported recently by Jansen *et al.*²⁰ A discussion of this subject is in a forthcoming paper. The comparatively low H-atom concentration close to the surface for a 1.0-mm filament diameter may be due to the 170 K lower filament temperature. Compared with Fig. 5, a temperature difference of 170 K alone may lead to a difference in H-atom concentrations of a factor of ~ 2 . Qualitatively, the measured profiles reflect the competition between H-atom production at and diffusion from the boundary layer; this effect may deserve further investigation in the future.

Another parameter of interest for optimization of a filament assisted CVD process is the wire material used. Figure 7 shows concentration profiles for two filament materials. The diameter was 2 mm and the temperature 2700 K in both cases. The experiment was performed at 30 mbar and 5% CH $_4$ addition. It can be seen that at least at small distances, tantalum seems to be more efficient in terms of H-atom production than iridium. In the case of iridium, the significantly smaller signal at 1 mm compared with 2-mm distance from the filament seems unreasonable; however, the effect is reproducible. A possible explanation²¹ could be that this decrease was caused by a higher quenching rate due to evaporated material or collisions with charged particles near the wire rather than by a lower atom concentration. To examine this effect more closely, the best approach is to determine quenching rates from lifetime measurements at lower pressures.

The effect of CH $_4$ addition on hydrogen atom con-

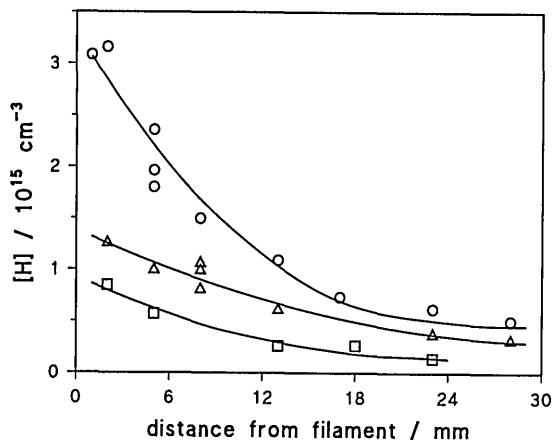


Fig. 6. Radial concentration profiles for different filament diameters: tantalum wire, $p = 30$ mbar, 5% CH_4 : \circ , 2-mm diameter, $T = 2700$ K; Δ , 1-mm diameter, $T = 2530$ K; \square , 0.3-mm diameter, $T = 2700$ K.

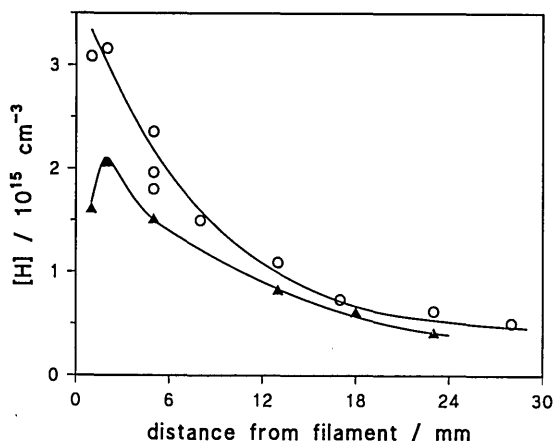


Fig. 7. Radial concentration profiles for different filament materials. Diameter, 2 mm; $p = 30$ mbar, CH_4 addition 5%: \circ , tantalum; Δ , iridium.

centrations is another interesting issue. In diamond CVD experiments, it is empirically found that best results are obtained with very low methane concentrations, usually of the order of 1%. We found initially that on addition of up to 5% of methane, which is comparable to the hydrogen atom concentrations, the effect on the H-atom concentrations was very small. This is illustrated in Fig. 8 where H-atom concentrations are shown as a function of CH_4 volume fractions. The weak effect of CH_4 addition is an interesting observation since it could be expected that H-atoms are consumed rapidly by the reaction with CH_4 , which has a relatively high rate coefficient²² at the high gas temperatures in the vicinity of the filament.

It can be seen that surface effects influenced the formation of hydrogen atoms in this experiment, since the concentrations remained on a low level directly after termination of CH_4 addition, as indicated by the solid square. A similar effect was observed for a tungsten filament; for iridium no significant change of the H-atom production efficiency after addition of methane could be observed. Also, on addition of CH_4 , the

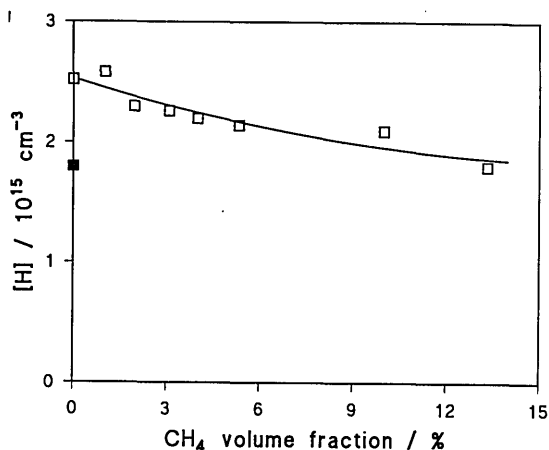


Fig. 8. H-atom concentrations as a function of CH_4 mixture fraction: $p = 30$ mbar; tantalum filament, 2-mm diameter; distance from filament, 4.4 mm; \blacksquare , taken immediately after termination of CH_4 addition.

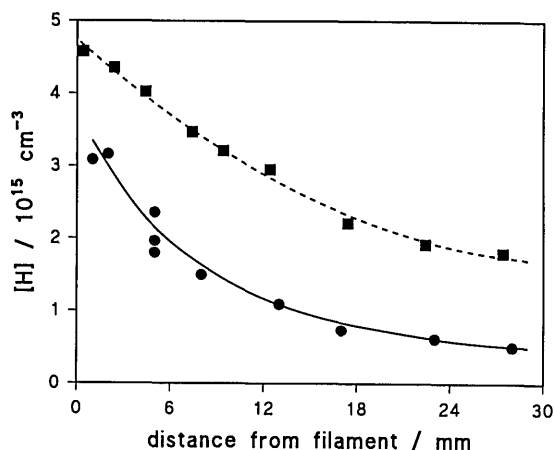


Fig. 9. Effect of CH_4 addition on H atom profiles; tantalum wire, 2-mm diameter, $p = 30$ mbar; \blacksquare , 0% CH_4 , filament temperature, 2620 K; \bullet , 5% CH_4 , filament temperature, 2700 K.

H-atom signal did not change immediately, as would be expected in the case of a gas phase reaction. Instead, it reached a constant value only after 2–10 min at $p = 30$ mbar, depending on wire diameter and material. Supplementary analysis of the tantalum filament using an electron-beam microprobe showed that after exposure to CH_4 a TaC layer several microns thick was formed on the surface. Temperature measurements showed that, as a consequence of the formation of this layer, the wire temperature changed even if the electrical power remained approximately constant. In the case of a tantalum filament, the temperature increased by 160° , whereas the power varied only by 1%. This temperature change may lead to a higher hydrogen dissociation rate (see Fig. 5), which may in turn explain the relatively small decrease of hydrogen atom concentrations on the addition of CH_4 . In contrast, Fig. 9 shows radial concentration profiles with and without CH_4 at approximately equal temperatures. It can be seen that with 5% methane, the H-atom concentrations are significantly lower and de-

crease more rapidly with increasing distance from the filament possibly due to the reaction with methane. These observations lead to the conclusion that the response of the filament material to reactive gas environments in a CVD process is an additional point of concern besides the gas phase and substrate surface effects.

The results of this study can be compared to modeled H-atom concentrations on the basis of measured stable species concentrations under similar reactor pressure and filament temperature.²³ Our concentrations agree with those in Ref. 23 within a factor of ~ 2 – 3 , which is a relatively good agreement considering our experimental uncertainty of a factor of ~ 2 . There is also good agreement in the decrease of H-atom concentrations at 3–5 mm from the filament on the addition of CH₄. In Ref. 23 the concentrations decrease by a factor of 0.54 from 1 to 7% CH₄, whereas we find a factor of 0.5 when going from 0 to 5% CH₄.

IV. Conclusions

The applicability of two-photon laser-induced fluorescence as a diagnostic tool in a CVD process has been demonstrated. Quantitative concentration measurements of hydrogen atoms with high spatial resolution were performed for a variety of experimental conditions, using a calibration technique which relates H-atom fluorescence signals to those from an independent reference system. The results may be incorporated in the development of chemical-kinetic models, which can be useful to obtain a better understanding of the complex kinetic processes associated with diamond CVD processes. Since laser-based optical detection techniques are available for a variety of species relevant in a CVD environment, e.g., CH₄, C₂H₂, CH₃, CH, H, O, or OH, it is basically possible to obtain a large set of experimental data for different processes to put the development of the above mentioned models on a broader basis.

The authors are indebted to J. Bittner for calculation of Doppler corrections at different temperatures and to U. Bringmann for technical support.

References

1. J. C. Angus and C. C. Hayman, "Low-Pressure, Metastable Growth of Diamond and 'Diamondlike' Phases," *Science* **241**, 913–921 (1988).
2. K. E. Spear, "Diamond-Ceramic Coating of the Future," *J. Am. Ceram. Soc.* **72**, 171–191 (1989).
3. M. Frenklach, "The Role of Hydrogen in Vapor Deposition of Diamond," *J. Appl. Phys.* **65**, 5142–5149 (1989).
4. F. G. Celii, P. E. Pehrsson, H.-t. Wang, and J. E. Butler, "Infrared Detection of Gaseous Species During the Filament-Assisted Growth of Diamond," *Appl. Phys. Lett.* **52**, 2043–2045 (1988).
5. S. J. Harris, A. M. Weiner, and T. A. Perry, "Measurement of Stable Species Present During Filament-Assisted Diamond Growth," *Appl. Phys. Lett.* **53**, 1605–1607 (1988).
6. F. G. Celii and J. E. Butler, "Hydrogen Atom Detection in the Filament-Assisted Diamond Deposition Environment," *Appl. Phys. Lett.* **54**(11), 1031–1033 (1989).
7. U. Meier, K. Kohse-Hoinghaus, and T. Just, "H and O Atom Detection For Combustion Applications: Study of Quenching and Laser Photolysis Effects," *Chem. Phys. Lett.* **126**, 567–573 (1986).
8. J. Bittner, K. Kohse-Hoinghaus, U. Meier, S. Kelm, and T. Just, "Determination of Absolute H Atom Concentrations in Low-Pressure Flames by Two-Photon Laser-Excited Fluorescence," *Combust. Flame* **71**, 41–50 (1988).
9. U. Meier, J. Bittner, K. Kohse-Hoinghaus, and T. Just, "Discussion of Two-Photon Laser-Excited Fluorescence as a Method for Quantitative Detection of Oxygen Atoms in Flames," in *Twenty-Second Symposium (International) on Combustion* (Combustion Institute, Pittsburgh, PA, 1988), pp. 1887–1896.
10. J. Bittner, K. Kohse-Hoinghaus, U. Meier, and T. Just, "Quenching of Two-Photon-Excited H(3s,3d) and O(3p³P_{2,1,0}) Atoms by Rare Gases and Small Molecules," *Chem. Phys. Lett.* **143**, 571–576 (1988).
11. U. Meier, K. Kohse-Hoinghaus, L. Schafer, and C.-P. Klages, "H Atom Concentration Measurement by Two-Photon LIF Near a Heated Filament in a Hydrogen Environment," in *Technical Digest, Topical Meeting on Laser Applications to Chemical Analysis* (Optical Society of America, Washington, DC, 1990), Vol. 2, pp. 100–102.
12. L. Schafer, U. Bringmann, C.-P. Klages, U. Meier, and K. Kohse-Hoinghaus, "Hydrogen Dissociation at Hot Filaments: Determination of Absolute Atomic Hydrogen Concentrations," to be presented at the NATO Advanced Study Institute on Diamonds and Diamond-Like Coatings, Il Ciocco Castelvechio Pascoli, Italy, 22 July–3 Aug. 1990 and manuscript in preparation.
13. Bo-nian Dai and P. Lambropoulos, "Selective Ionization: Effects of Power Broadening, Laser Bandwidth, and Interaction Time on Selectivity," *Phys. Rev. A* **34**, 3954 (1986).
14. J. Bittner, "Bestimmung von absoluten H- und O-Atomkonzentrationen mit Laser-Induzierter Fluoreszenz (LIF) auf der Basis von Mehrphotonentechniken in Flammen," Ph.D. Thesis, DLR/U. Heidelberg (Sept. 1989).
15. P. Lambropoulos, University of Southern California, Los Angeles; private communication (1987).
16. J. E. M. Goldsmith, "Two-Photon-Excited Stimulated Emission from Atomic Hydrogen in Flames," *J. Opt. Soc. Am. B* **6**, 1979–1985 (1989).
17. J. E. M. Goldsmith, "Two-Photon-Excited Stimulated Emission from Atomic Hydrogen in Flames," in *Technical Digest, Topical Meeting on Laser Applications to Chemical Analysis* (Optical Society of America, Washington, DC, 1990), Vol. 2, pp. 103–105.
18. E. Schnedler, "Description of Tungsten Transport Processes in Inert Gas Incandescent Lamps," *Philips J. Res.* **38**, 224–235 (1983).
19. K. Blodgett and I. Langmuir, "Accommodation Coefficient of Hydrogen; a Sensitive Detector of Surface Films," *Phys. Rev.* **40**, 78–104 (1932) and references therein.
20. F. Jansen, I. Chen, and M. A. Machonkin, "On the Thermal Dissociation of Hydrogen," *J. Appl. Phys.* **66**, 5749–5755 (1989).
21. J. B. Jeffries, SRI International; private communication (1990).
22. P. Roth and T. Just, "Atom-Resonanzabsorptionsmessungen beim thermischen Zerfall von Methan hinter Stosswellen," *Ber. Bunsenges. Phys. Chem.* **79**, 682–686 (1975).
23. S. J. Harris and A. M. Weiner, "Effects of Oxygen on Diamond Growth," *Appl. Phys. Lett.* **55**, 2179–2181 (1989).